

**Optical enhancement of NMR signals in CdTe**

Isaac J. H. Leung and Carl A. Michal\*

*Department of Physics and Astronomy, University of British Columbia, 6224 Agricultural Road, Vancouver, British Columbia, Canada, V6T 1Z1*

(Received 28 November 2003; revised manuscript received 19 April 2004; published 29 July 2004)

We report the direct inductive detection of optically enhanced nuclear magnetic resonance (NMR) signals from  $^{123}\text{Te}$ ,  $^{125}\text{Te}$ ,  $^{111}\text{Cd}$ , and  $^{113}\text{Cd}$  in a single crystal of CdTe under excitation with near band-gap illumination. The illumination wavelength, power and sample temperature dependence of the excitation are presented. From a comparison of the amplitudes of the NMR signals observed from the different nuclear species, we conclude that the optical enhancement of the nuclear spin polarization in the bulk semiconductor is not consistent with a mechanism that relies on spin diffusion, but may be consistent with a recently proposed mechanism involving the direct polarization of the bulk from optically excited excitons. Significantly enhanced NMR signals are observed at temperatures as high as 100 K.

DOI: 10.1103/PhysRevB.70.035213

PACS number(s): 76.70.Fz, 82.56.-b, 81.05.Dz

**I. INTRODUCTION**

The production, control, and detection of spin polarization in solids has become a topic of increasing importance for both scientific and technological applications. The use of nuclear spins in solids as qubits for quantum computation<sup>1-3</sup> and the emerging field of “spintronics”<sup>4</sup> are two examples where such manipulation of spin degrees of freedom are crucial. Of interest in our laboratory is the generation of non-equilibrium nuclear spin polarization in solids by optical pumping. Such polarization has been proposed as the basis of a nuclear magnetic resonance (NMR) signal enhancement technique for biological samples overlaid on semiconductor substrates.<sup>5</sup> This technique, known as transferred optically pumped NMR (TOPNMR), has not yet been experimentally demonstrated.

The direct inductive detection of optical polarization of nuclear spins was first performed by Lampel in silicon,<sup>6</sup> and has been most studied in GaAs.<sup>5</sup> More recently, optical polarization of nuclear spins has been observed in InP,<sup>5,7,8</sup> CdS,<sup>9</sup> and CdSe.<sup>10</sup> It was suggested that GaAs would not be a suitable substrate for TOPNMR because all of the abundant nuclear spin species have large quadrupolar moments that, at the surface, would interfere with polarization transfer. InP was suggested as an alternative, as  $^{31}\text{P}$  is 100% abundant, has a relatively large nuclear gyromagnetic ratio, and has spin-1/2.

CdTe is a II-VI semiconductor that has long been used in optoelectronic devices due to its favorable optical properties and near-infrared direct gap.<sup>11</sup> CdTe contains four spin-1/2 nuclear species in reasonable abundance:  $^{123}\text{Te}$ (0.91%),  $^{125}\text{Te}$ (7.14%),  $^{111}\text{Cd}$ (12.8%), and  $^{113}\text{Cd}$ (12.22%), but optically pumped nuclear spin polarization in CdTe has not, to our knowledge, been observed. In this work we present the wavelength, intensity, and temperature dependence of directly detected optical polarization of nuclear spins in undoped, high-resistivity CdTe.

The process by which optically pumped nuclear spin polarization is generated is described in the literature as the result of Overhauser cross relaxation of photoexcited elec-

trons trapped at shallow defects.<sup>12-16</sup> In this description, nuclear spins in the bulk semiconductor are polarized by the diffusion of spin polarization from localized optical pumping sites,<sup>17</sup> presumably defects or dopants. More recently it has been proposed<sup>18</sup> that polarization arising from cross relaxation from mobile excitons may dominate the bulk polarization. The variety of isotopic abundances of the nuclear spin species in CdTe, along with the dependence of the efficiency of spin diffusion with isotopic abundance, provide an opportunity to test the two mechanisms. We find that the signal intensities are not consistent with a mechanism where nuclear spin diffusion is required to polarize the bulk.

**II. EXPERIMENTAL SETUP**

All measurements were performed on a single undoped crystal of CdTe measuring  $2.1 \times 4.8 \times 1.1 \text{ mm}^3$  (obtained from University Wafer, South Boston, MA, USA, Lot No. 6796). The resistivity of the sample was specified by the manufacturer to be  $>10^9 \Omega \text{ cm}$ . Based on a carrier mobility of  $\approx 1000 \text{ cm}^2/\text{V s}$  in compensated CdTe samples of similar resistivity,<sup>19,20</sup> we estimate the carrier concentration to be  $<6 \times 10^6 \text{ cm}^{-3}$ .

Experiments were carried out in an 8.4 T magnet from Oxford Instruments using a homebuilt NMR spectrometer<sup>21</sup> and a Janis Research (Supertran) continuous-flow cryostat that had been fitted with the rotary motion feedthroughs, coaxial cables, and cryogenic capacitors required for operation as a low-temperature NMR probe. The top and bottom surfaces of the CdTe crystal, which had been polished by the manufacturer, were cleaned with methanol before mounting using Apiezon N grease on a piece of  $\text{Al}_2\text{O}_3$  that provided thermal contact to, but electrical insulation from, the probe's cold finger. Grooves were cut into the  $\text{Al}_2\text{O}_3$  substrate to allow the NMR coil to encircle the sample. The same NMR coil was used for all measurements. The sample temperature was controlled with a Lakeshore Model 340 temperature controller (Lakeshore Cryotronics, Westerville, OH, USA) that monitored a Cernox RTD (Lakeshore) mounted inside the cold finger.

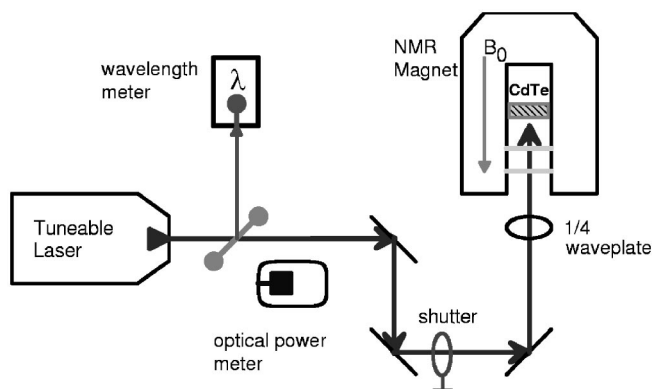


FIG. 1. Schematic diagram of the experimental setup. The optical power meter is inserted into the optical path prior to the experiment and removed before the optical excitation and NMR acquisition.

A 1 W tunable Ti:sapphire laser (899-LC, Coherent Inc, Santa Clara, CA, USA) was used for optical excitations. Laser output power and wavelength were measured at the source with a Coherent Fieldmaster GS power meter and a Coherent Wavemate wavelength meter. A series of mirrors was used to steer the beam through a zero-order 1/4 wave plate and two clear quartz windows, and onto the sample as shown in Fig. 1. The beam diameter at the target was approximately 5 mm. Optical loss after the three mirrors was measured to be less than 1%.

A spectrometer-controlled shutter provided control of the irradiation time. All spectra, except as noted, were acquired following 10 s of dark time so that the electron system could return to the ground state. No change in the signal amplitude or line shape was observed if the sample remained irradiated during acquisition, consistent with similar measurements on GaAs using a similar setup.<sup>18</sup>

The sample temperature increase was estimated, with 300 mW laser output, to be less than 2 K during a complete acquisition cycle. This was determined by placing a second Cernox RTD (Lakeshore) inside the cryostat immediately adjacent to the CdTe crystal on the same piece of Al<sub>2</sub>O<sub>3</sub>. The RTD was covered to avoid exposure to laser light.

The pulse sequence used for acquisition of the NMR signals was

$$\text{SAT} - \tau_{\text{light}} - \tau_{\text{dark}} - \text{ACQ},$$

where SAT is a presaturation sequence consisting of a series of fifty 90° pulses separated by 1 ms.  $\tau_{\text{light}}=120$  s,  $\tau_{\text{dark}}=10$  s, except where noted, and ACQ represents the acquisition of the free induction decay following a 90° pulse. A typical 90° pulse duration was 6  $\mu$ s. Signals were averaged over four identical acquisition sequences, except where noted.

### III. RESULTS AND DISCUSSION

#### A. Wavelength dependence of optically enhanced NMR

The wavelength dependence of the optically enhanced <sup>125</sup>Te NMR signal at 10 K is shown in Fig. 2. Without opti-

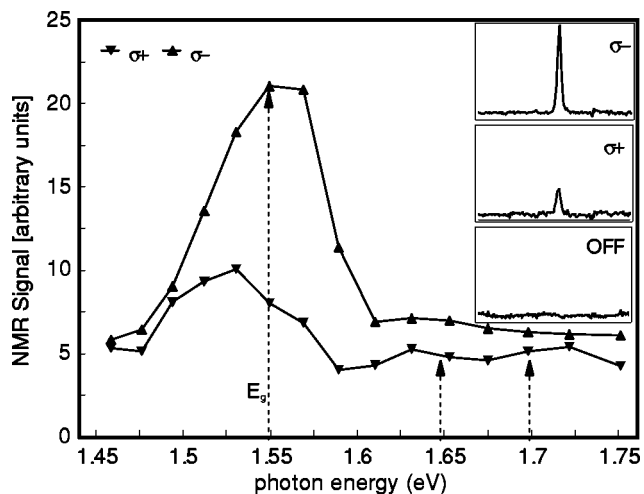


FIG. 2. Optical enhancement of <sup>125</sup>Te NMR signals at a sample temperature of 10 K and 300 mW laser power. The lines connecting the points are guides to the eye. The arrow indicating  $E_g$  is approximate (based on Ref. 22). The two other arrows indicate the estimated optical band gaps of the wurtzite form of CdTe at 10 K, based on experimental data at 2 K.<sup>23</sup> The insets show NMR spectra for right ( $\sigma^-$ ) and left ( $\sigma^+$ ) circularly polarized light exposure at  $\sim 1.56$  eV, as well as for  $\tau_{\text{light}}=0$ ,  $\tau_{\text{dark}}=121$  s. The total bandwidth shown in the insets is 40 kHz and the full width at half maximum of the signal is approximately 1.5 kHz.

cal pumping, there is no visible NMR signal under the same conditions. The peak in the observed enhancement occurs very close to the band gap of CdTe, given in eV by<sup>22</sup>

$$E_g = 1.56 - 4.1 \times 10^{-4} T, \quad (1)$$

which at 10 K corresponds to approximately 1.55 eV (797 nm).

Measurements of the optically enhanced NMR signals acquired from <sup>125</sup>Te, <sup>111</sup>Cd, and <sup>113</sup>Cd at 78 K are shown in Fig. 3. The peak in enhancement for  $\sigma^-$  polarized light is again in agreement with the band gap of CdTe at 78 K, which is calculated from Eq. (1) to be 1.53 eV (810 nm).

Two minor peaks in the NMR signals are visible in some curves of Figs. 2 and 3 at photon energies above the band gap. Additional peaks might be expected at energies corresponding to exciting higher exciton levels,<sup>24</sup> surface phonon modes,<sup>25</sup> or spaced by the LO phonon energy.<sup>26</sup> However, the spacing between the features we observe and the band gap is more than an order of magnitude smaller than would be expected for either of the first two possibilities, and much too large to be explained by the 21 meV (Ref. 27) of LO phonons in CdTe. The  $P_{1/2}$  splitoff band is approximately 0.9 eV ( $[\Gamma_9^v - \Gamma_6^c]$ ) higher in energy,<sup>28</sup> corresponding to approximately 510 nm, and is out of the range of excitation energies accessible with our laser.

One possibility is that these two peaks are due to the existence of a wurtzite (hexagonal) phase in, or at the surface of, the crystal. The energy of these two peaks shows good correspondence to photoluminescence measurements on the band gap of CdTe in the wurtzite phase,<sup>23</sup> which also shows two peaks ( $[\Gamma_9^v - \Gamma_7^c]$  and  $[\Gamma_7^v - \Gamma_7^c]$ ) with similar energy sepa-

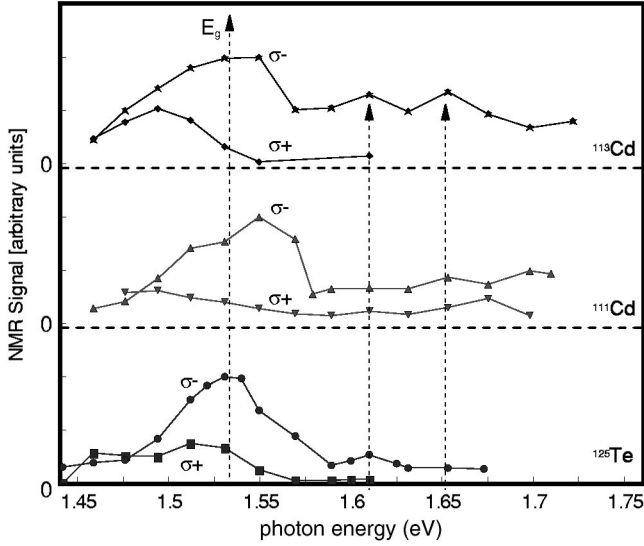


FIG. 3. Wavelength dependence of the optically enhanced NMR signals of  $^{125}\text{Te}$ ,  $^{111}\text{Cd}$ , and  $^{113}\text{Cd}$  in CdTe at 78 K under illumination with 300 mW  $\sigma^+$  or  $\sigma^-$  light. The lines connecting the points are guides to the eye. The plots are offset for clarity. The arrow indicating the bandgap  $E_g$  is approximate. The two other arrows indicate the estimated optical band gaps of the wurtzite form of CdTe at 78 K, based on experimental data at 2 K.<sup>23</sup>

ration. In II-VI semiconductor materials, the  $\pm\{111\}$  facet of the zincblende phase and the  $\pm(0001)$  facet of the wurtzite phase are atomically matched. The existence of multiple phases in a single crystal (polytypism) has been observed in several types of semiconductors<sup>29–33</sup> and, specifically, has been shown to occur in CdTe,<sup>34</sup> depending on the crystal growth conditions. Relatively small changes in temperature and other conditions during crystal growth can be sufficient to induce polytypism, and this has recently been exploited to control the manufacturing of polytypic CdTe crystals.<sup>35</sup>

Measurements on GaN (Ref. 30) suggest that the second phase may occur at the crystal surface. One surface of the CdTe crystal was etched in HCl for 10 min, followed by a rinse in de-ionized water. The sample was then immediately placed into the cryostat and pumped out to a vacuum of better than  $10^{-6}$  Torr. The secondary feature at 1.61 eV in the resulting  $^{125}\text{Te}$  photon energy spectrum is approximately half the size of that in the lower curve in Fig. 3, suggesting that the origin of the secondary peaks is related to a feature of the crystal surface, consistent with the existence of a wurtzite phase there.

The largest NMR enhancements are observed with  $\sigma^-$  irradiation and are absorptive. This is consistent with the negative electronic  $g$  factor<sup>36</sup> and negative gyromagnetic ratio for all four nuclear spin species (the static field,  $B_0$  in our magnet points down).

We expect the sign of the nuclear spin polarization to invert as the excitation is changed from  $\sigma^-$  to  $\sigma^+$ , however, no such inversion occurs and the signals are always absorptive. This lack of inversion was also observed in a Be-doped GaAs sample<sup>15</sup> and was attributed to the efficiency of electron-spin relaxation or a large difference in recombination rates between spin-up and -down photoelectrons.

## B. Spin species dependence

A key feature of a recently proposed mechanism for the optical polarization of nuclear spins in the bulk<sup>18</sup> is that it does not involve the transport of nuclear spin polarization by spin diffusion. This is in contrast to the previous description of such bulk polarization.<sup>12–17</sup> Measurement of the optically pumped nuclear spin polarization for the various NMR active isotopes in CdTe allows a comparison with predictions based on each of these models. We begin with a calculation of the relative signal amplitudes expected from the different spin species for the two mechanisms.

In the newly proposed mechanism,<sup>18</sup> nuclear spins in the bulk semiconductor are directly polarized by contact hyperfine coupling to mobile excitons. The existence of free excitons in CdTe has been previously observed in photoluminescence experiments.<sup>37,38</sup> The magnitude of this coupling can be expressed as<sup>39</sup>

$$A_{hf} = \frac{8\pi}{3} \gamma_n \gamma_e \hbar^2 |\psi(0)|^2, \quad (2)$$

where  $\gamma_n$  and  $\gamma_e$  are the gyromagnetic ratios of the nucleus and electron, respectively, and  $|\psi(0)|^2$  is the wave-function density of the electron at the nucleus of interest.

In the initial rate regime, the observed signal will be proportional to the relaxation rate,  $(A_{hf}^2)$ , the abundance  $A$  of the nuclear spin species, as well as an additional factor  $\gamma_n$ , to account for the increased signal observed at higher resonance frequencies. We thus expect the amplitude of the detected NMR signal to be given by

$$S \propto \gamma_n^3 A |\psi(0)|^4, \quad (3)$$

where we have dropped factors that are common for all of the different nuclear spin species.

In the case where the bulk semiconductor is polarized by spin diffusion from fixed sites, we expect, for our illumination time of 120 s, that a small region around each fixed source will be in quasiequilibrium, where<sup>8</sup>

$$\frac{1}{T_n} = \mp \frac{\gamma_e}{\gamma_n} \left( \frac{1}{T_e} - \frac{1}{T} \right), \quad (4)$$

in which  $T_n$  and  $T_e$  are the nuclear and electron spin temperatures, respectively,  $T$  is the lattice temperature, and the upper sign should be taken if the electron  $g$  factor and nuclear  $\gamma$  have the same sign. In this quasiequilibrium, the fractional polarization of all spin species in the core, proportional to  $\gamma_n/T_n$ , is equal. The rate of diffusion of spin polarization from the core then depends upon the abundance of the nuclear spin species as well as on  $\gamma_n$ .

For a fixed lattice geometry containing a single, 100% abundant spin species, the spin diffusion coefficient  $D$  may be written<sup>40</sup>

$$D = c \frac{\gamma^2}{r}, \quad (5)$$

where  $c$  is a constant of order unity, and  $r$  is the nearest-neighbor distance.

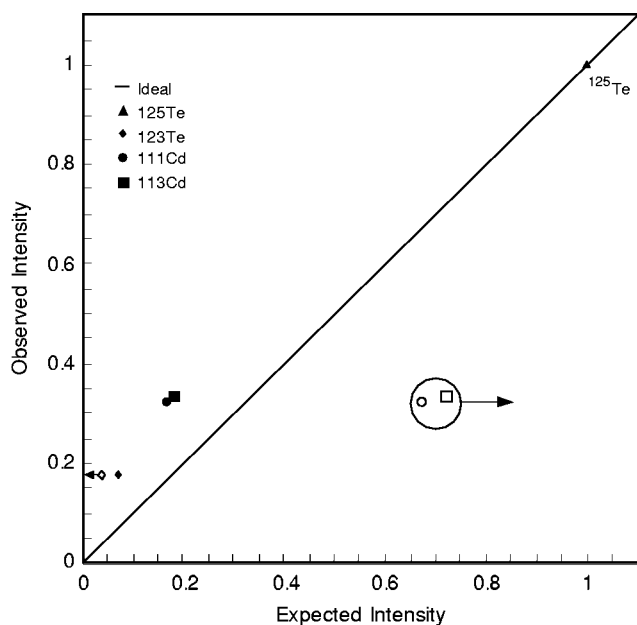


FIG. 4. Spin species dependence of NMR signal amplitudes. The amplitude of the observed NMR signals are plotted against those expected based on two different bulk polarization mechanisms. All signals were normalized to the maximum observed value for  $^{125}\text{Te}$  at the same experimental setting of 300 mW laser power at 1.55 eV (800 nm). Open symbols show the expected value for the model incorporating spin diffusion. Closed symbols are from the direct polarization model. The horizontal arrows show the direction of change expected if the additional effects described in the text are included in the diffusion coefficient. The straight line shown has a slope of one.

Ignoring heteronuclear interactions for the moment, a mean-field treatment for a diluted lattice would lead to the expectation that  $D \propto \gamma_n^2 A^{1/3}$ . At low abundance,  $D$  should fall below the mean-field value as polarization gets trapped in clusters of nearby spins, as accounted for by including exponential cutoffs<sup>41</sup> or nearest-neighbor restrictions<sup>42</sup> in numerical simulations of spin diffusion.

In the regime where neighboring polarization sources are far apart compared to  $(Dt)^{1/2}$ , the total spin polarization in the region surrounding a single pumping site is proportional to  $D$ . This is obtained by solving the diffusion equation with a constant boundary condition, and then integrating the total intensity in all space. Solutions of the one-dimensional diffusion equation produce error functions, which when integrated show a  $\sqrt{Dt}$  dependence, but in the isotropic three-dimensional case, the solution yields a linear dependence on  $D$ . Adopting the mean-field prediction for  $D$ , we expect the signal to be given by

$$S \propto (\gamma_n^2 A^{1/3}) \gamma_n A. \quad (6)$$

A comparison of the NMR signals observed from all four nuclear spin species with the predictions of these two mechanisms is shown in Fig. 4. The values of  $|\psi(0)|^2$  used are those calculated using localized orbital methods<sup>43</sup> (0.4 for Te and 0.22 for Cd).

These calculations do not account for the expected  $\gamma^{1/2}$  degradation in signal intensity expected due to declining coil quality factor with frequency. This effect was ignored because no measurable difference in quality factor was observed when the circuit was examined at each of the NMR frequencies with an rf sweep generator. The principle effect of including this factor in the expected intensity calculations may be visualized by moving the abscissa of the  $^{125}\text{Te}$  point from 1.0 to 0.82. The abscissa of the  $^{123}\text{Te}$  points would also move to the left very slightly, by approximately 10% of their values.

The spin diffusion coefficient will be modified from the mean-field prediction by the clustering effect noted above and also by the suppression of diffusion by couplings to neighboring spins of different  $\gamma$ .<sup>44</sup> We take the  $^{125}\text{Te}$  signal as a baseline and compare the abundance and environment of the other nuclear species to it. The two Cd isotopes have similar  $\gamma$ , similar abundance, and similar environment with respect to the density and gyromagnetic ratios of neighbors. Because the Cd isotopes are the most abundant and have the fewest neighbors with nuclear spins, we expect that compared to the Te species, their diffusion coefficients will be least affected by both of the two effects described.  $^{123}\text{Te}$ , on the other hand, is the least abundant, and has the largest number of neighbors with nuclear spins, and so it should be affected the most by both effects. These predictions are represented by the arrows in Fig. 4, that show that the model incorporating spin diffusion can only fit the data even more poorly if the neglected effects are taken into account. Incorporating the expected degradation of signal due to declining coil quality factor with frequency would improve the fit to the exciton model and further worsen the fit to the spin diffusion model. A linear regression based on Eq. (3) provides  $R^2=0.86$ , while a similar regression based on Eq. (6) found  $R^2=0.60$ , providing strong evidence that the polarization of the bulk semiconductor does not depend on nuclear spin polarization from fixed pumping sites.

### C. Dependence on optical power and sample temperature

The dependence of the amplitude of the NMR signal acquired as a function of the incident laser power is shown in Fig. 5. The dependence of the signal amplitude on optical power has been predicted<sup>5</sup> to be

$$S(P_{in}) = S_{max} \int_0^{z_d} \left[ 1 - \exp\left(-\frac{P_{in} e^{-z/z_0}}{P_s}\right) \right] dz + S_{bulk}, \quad (7)$$

where  $z_0$  is the absorption depth in the sample ( $1.15 \mu\text{m}$ <sup>45</sup>),  $z_d$  is the depth of the sample,  $P_{in}$  is the incident optical power density,  $P_s$  is the saturation power density,  $S_{bulk}$  is the signal arising from thermal relaxation in the bulk semiconductor substrate below the optically pumped layer, and  $S_{max}$  is the signal expected from the optically pumped layer if fully polarized. This equation does not include contributions from photobleaching, reabsorption of luminescence, or differential absorption of different light polarization states.

A fit of Eq. (7) to the data, assuming  $S_{bulk}=0$  and  $z_d=\infty$ , yields a saturation power  $P_s \approx 600 \text{ mW/cm}^2$ , somewhat

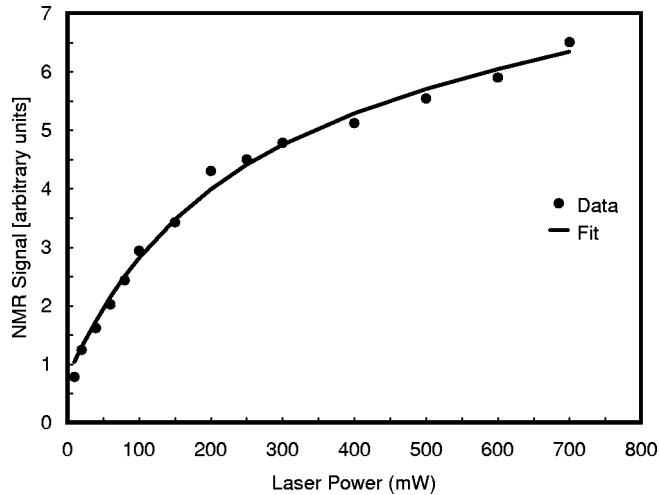


FIG. 5. Laser power dependence of optically enhanced  $^{125}\text{Te}$  NMR signals. The photon energy is fixed at 1.53 eV with  $\sigma^-$  polarization and a sample temperature of 78 K. Circles are data points, the line is the best least-squares fit to Eq. (7) as described in the text.

higher than the 60–123 mW/cm<sup>2</sup> observed in InP<sup>5</sup> and GaAs.<sup>46</sup>

The dependence of the optically enhanced NMR signal on temperature is shown in Fig. 6. As expected, the optical enhancement diminishes rapidly as the temperature is raised, however, we are able to observe an enhancement in signal above 100 K in both  $^{125}\text{Te}$  and  $^{111}\text{Cd}$  with the laser tuned to 600 mW at 800 nm. A significant NMR signal enhancement was still visible on  $^{111}\text{Cd}$  even at 120 K.

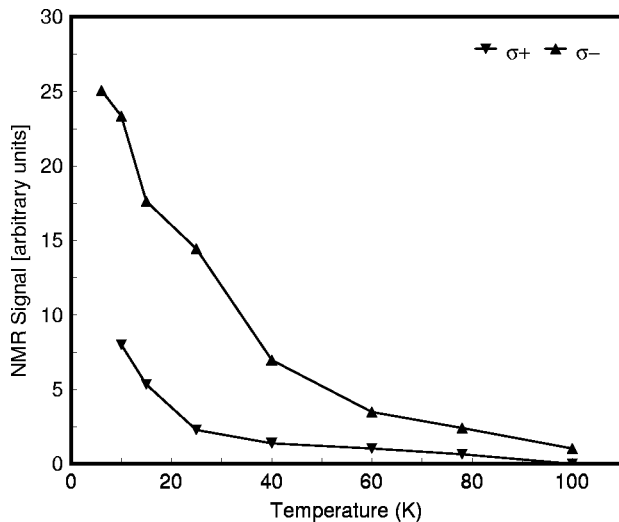


FIG. 6. Temperature dependence of optical enhancement of  $^{125}\text{Te}$  NMR signal. The laser power was fixed at 500 mW, while the photon energy was varied from 1.55 to 1.51 eV to match the expected band gap at each temperature.

#### D. Maximum polarization and dependence on irradiation time

In order to estimate the total nuclear spin polarization that could be excited, the amplitude of the maximum NMR signal following a long period of optical excitation (2400 and 2500 s for 78 K and 10 K, respectively) was compared to reference spectra acquired from the same sample in thermal equilibrium at room temperature.

At 78 K, the  $^{125}\text{Te}$  NMR signal displayed an approximately exponential time dependence, with a relaxation time of  $\sim 1000$  s. In the absence of optical excitation, the  $^{125}\text{Te}$   $T_1$  at 78 K is  $>10\,000$  s. The ratio of the optically pumped signal at 78 K to the thermal equilibrium signal at 290 K was approximately 6.7, while the number of nuclei contributing to the optically pumped signal is approximately 956 times smaller than that of the thermal equilibrium signal because of the 1.15  $\mu\text{m}$  penetration depth of the light. The nuclear spin temperature under these conditions is estimated at  $T_n \approx 0.04$  K (spin polarization  $p = (N_\uparrow - N_\downarrow) / (N_\uparrow + N_\downarrow) = 0.06$ ).

At a sample temperature of 10 K, with continuous irradiation of 500 mW of 1.55 eV light, we found a  $^{125}\text{Te}$  relaxation time of  $\sim 1900$  s, and a maximum signal corresponding to a nuclear spin polarization  $p = 0.33$  or a nuclear spin temperature of  $T_n \approx 0.008$  K.

These estimates do not include the effects of excitonic diffusion. The exciton diffusion length is expected to be on the order of 1  $\mu\text{m}$  (Ref. 47) at 78 K. Inclusion of these effects would increase the apparent penetration depth and lower the polarization estimates by a factor of 1.5–2.

#### IV. CONCLUSION

We have reported the detection of optically enhanced NMR signals from  $^{111}\text{Cd}$ ,  $^{113}\text{Cd}$ ,  $^{123}\text{Te}$ , and  $^{125}\text{Te}$  in CdTe. Measurements of the magnitude of the signal enhancement show a peak response at a photon energy corresponding to the band gap of the cubic form of CdTe, while two minor peaks in the response show correspondence to the band-gap energies of the hexagonal form. This may be explained by the presence of polytypism in the CdTe crystal used. The observed enhancements are detectable even at relatively high temperatures, above 77 K.

Comparisons of the relative strengths of the NMR signals of the Cd and Te nuclei do not appear to be consistent with a mechanism for polarizing the bulk nuclear spins that depends on spin diffusion, rather the amplitudes of the NMR signals observed from the four observable spin species are much better predicted by a model incorporating direct polarization of the nuclear spins in the bulk by optically excited electrons or excitons.

#### ACKNOWLEDGMENTS

This work was supported by grants from Research Corporation and the Natural Sciences and Engineering Research Council of Canada. We thank Matt Grinder for modifications to the cryostat and helpful conversations.

\*Electronic address: [michal@physics.ubc.ca](mailto:michal@physics.ubc.ca)

- <sup>1</sup>G. P. Berman, G. D. Doolen, P. C. Hammel, and V. I. Tsifrinovich, *Phys. Rev. B* **61**, 14 694 (2000).
- <sup>2</sup>G. P. Berman, G. D. Doolen, and V. I. Tsifrinovich, *Superlattices Microstruct.* **27**, 89 (2000).
- <sup>3</sup>J. M. Bao, A. V. Bragas, J. K. Furdyna, and R. Merlin, *Nat. Mater.* **2**, 175 (2003).
- <sup>4</sup>G. Zorpette, *IEEE Spectrum* **38**, 30 (2001).
- <sup>5</sup>R. Tycko, *Solid State Nucl. Magn. Reson.* **11**, 1 (1998).
- <sup>6</sup>G. Lampel, *Phys. Rev. Lett.* **20**, 491 (1968).
- <sup>7</sup>A. Patel, O. Pasquet, J. Bharatam, E. Hughes, and C. R. Bowers, *Phys. Rev. B* **60**, R5105 (1999).
- <sup>8</sup>C. A. Michal and R. Tycko, *Phys. Rev. B* **60**, 8672 (1999).
- <sup>9</sup>T. Pietrass and M. Tomaselli, *Phys. Rev. B* **59**, 1986 (1999).
- <sup>10</sup>N. T. Bagraev, L. S. Vlasenko, and R. A. Zhitnikov, *Sov. Phys. Solid State* **19**, 1956 (1977).
- <sup>11</sup>K. Zanio, *Semiconductors and Semimetals: Volume 13: Cadmium Telluride* (Academic, New York, 1978), Chap. V, p. 90.
- <sup>12</sup>R. Tycko and J. A. Reimer, *J. Phys. Chem.* **100**, 13 240 (1996).
- <sup>13</sup>C. Hermann and G. Lampel, *Ann. Phys. (Paris)* **10**, 1117 (1985).
- <sup>14</sup>M. I. D'yakonov and V. I. Perel', *Sov. Phys. JETP* **38**, 177 (1974).
- <sup>15</sup>T. Pietrass, A. Bifone, T. Room, and E. L. Hahn, *Phys. Rev. B* **53**, 4428 (1996).
- <sup>16</sup>P. L. Kuhns, A. Kleinhammes, T. Schmiedel, W. G. Moulton, E. Hughes, S. Sloan, P. Chabrier, and C. R. Bowers, *Phys. Rev. B* **55**, 7824 (1997).
- <sup>17</sup>D. Paget, *Phys. Rev. B* **25**, 4444 (1982).
- <sup>18</sup>A. K. Paravastu, S. E. Hayes, B. Schwickert, L. N. Dinh, M. Balooch, and J. A. Reimer, *Phys. Rev. B* **69**, 075203 (2004).
- <sup>19</sup>J. Franc, P. Hoschl, E. Belas, R. Grill, P. Hlidek, P. Moravec, and J. Bok, *Nucl. Instrum. Methods Phys. Res. A* **434**, 146 (1999).
- <sup>20</sup>D. Korbutyak, S. Krylyuk, P. Tkachuk, V. Tkachuk, N. Korbutjak, and M. Raransky, *J. Cryst. Growth* **197**, 659 (1999).
- <sup>21</sup>C. A. Michal, K. Broughton, and E. Hansen, *Rev. Sci. Instrum.* **73**, 453 (2002).
- <sup>22</sup>D. R. Lide, Ed., *Handbook of Chemistry and Physics*, 77th ed. (CRC, Boca Raton, FL, 1996), Chap. 12, pp. 12–98.
- <sup>23</sup>P. Lefebvre, T. Richard, J. Allegre, H. Mathieu, A. Combette-Roos, and W. Granier, *Phys. Rev. B* **53**, 15 440 (1996).
- <sup>24</sup>K. Watanabe and N. Miura, *J. Appl. Phys.* **88**, 4245 (2000).
- <sup>25</sup>H. M. Tutuncu, R. Miotto, and G. P. Srivastava, *Phys. Rev. B* **62**, 15 797 (2000).
- <sup>26</sup>C. B. la Guillaume, *J. Phys. Colloq.* **35**, C3 (1974).
- <sup>27</sup>M. Betz, G. Goger, A. Laubereau, P. Gartner, L. Banyai, H. Haug, K. Ortner, C. R. Becker, and A. Leitenstorfer, *Phys. Rev. Lett.* **86**, 4684 (2001).
- <sup>28</sup>A. V. Kimel, V. V. Pavlov, R. V. Pisarev, V. N. Gridnev, F. Ben-tivegna, and T. Rasing, *Phys. Rev. B* **62**, R10 610 (2000).
- <sup>29</sup>T. V. Timofeeva, V. N. Nesterov, R. D. Clark, B. Penn, D. Frazier, and M. Y. Antipin, *J. Mol. Struct.* **647**, 181 (2003).
- <sup>30</sup>H. Selke, V. Kirchner, H. Heinke, S. Einfeldt, P. Ryder, and D. Hommel, *J. Cryst. Growth* **208**, 57 (2000).
- <sup>31</sup>C.-Y. Yeh, Z. W. Lu, S. Froyen, and A. Zunger, *Phys. Rev. B* **46**, 10 086 (1992).
- <sup>32</sup>B. Gilbert, B. H. Frazer, H. Zhang, F. Huang, J. F. Banfield, D. Haskel, J. C. Lang, G. Srajer, and G. DeStasio, *Phys. Rev. B* **66**, 245205 (2002).
- <sup>33</sup>C. H. Park, B.-H. Cheong, K.-H. Lee, and K. J. Chang, *Phys. Rev. B* **49**, 4485 (1994).
- <sup>34</sup>J. Huerta, M. Lopez, and O. Zelaya-Angel, *J. Vac. Sci. Technol. B* **18**, 1716 (2000).
- <sup>35</sup>L. Manna, D. J. Milliron, A. Meisel, E. C. Scher, and A. P. Alivisatos, *Nat. Mater.* **2**, 382 (2003).
- <sup>36</sup>B. K. Meyer, A. Hofstaetter, U. Leib, and D. M. Hofmann, *J. Cryst. Growth* **184/185**, 1118 (1998).
- <sup>37</sup>G. Fonthal, L. Tirado-Mejia, J. Marin-Hurtado, H. Ariza-Calderon, and J. Mendoza-Alvarez, *J. Phys. Chem. Solids* **61**, 579 (2000).
- <sup>38</sup>S. H. Song, J. F. Wang, G. M. Lalev, L. He, and M. Isshiki, *J. Cryst. Growth* **252**, 102 (2003).
- <sup>39</sup>C. P. Slichter, *Principles of Magnetic Resonance* (Springer, Berlin, 1990), Chap. 4, p. 133.
- <sup>40</sup>I. J. Lowe and S. Gade, *Phys. Rev.* **156**, 817 (1967).
- <sup>41</sup>I. M. Nolden and R. J. Silbey, *Phys. Rev. B* **54**, 381 (1996).
- <sup>42</sup>D. K. Sodickson and J. S. Waugh, *Phys. Rev. B* **52**, 6467 (1995).
- <sup>43</sup>E. Erbarut, *Phys. Status Solidi B* **164**, 235 (1991).
- <sup>44</sup>C. Tang and J. S. Waugh, *Phys. Rev. B* **45**, 748 (1992).
- <sup>45</sup>S. Adachi, T. Kimura, and H. Suzuki, *J. Appl. Phys.* **74**, 3435 (1993).
- <sup>46</sup>S. E. Barrett, R. Tycko, L. N. Pfeiffer, and K. W. West, *Phys. Rev. Lett.* **72**, 1368 (1994).
- <sup>47</sup>M. J. Romero, T. A. Gessert, and M. M. Al-Jassim, *Appl. Phys. Lett.* **81**, 3161 (2002).